JOURNAL OF
CHEMICAL &
ENGINEERING
DATA

Article

pubs.acs.org/jced

Low-Pressure Adsorption Isotherms of Aromatic Compounds on Polyisobutylene Gel Measured on a Quartz Crystal Microbalance

Min-Jin Hwang, Wang Geun Shim, Dong-Wan Ryu, and Hee Moon*

Center for Functional Nano Fine Chemicals and School of Applied Chemical Engineering, Chonnam National University, Gwangju 500-757, South Korea

ABSTRACT: Adsorption equilibrium isotherms of benzene, toluene, and *p*-xylene on poly(isobutylene) (PIB) gel are experimentally measured at (293.15, 303.15, and 313.15) K on a quartz crystal microbalance to obtain very low-pressure adsorption data near the Henry's law region. This apparatus is very useful in measuring adsorption amounts on nonporous adsorbents, especially those with small surface areas such as PIB, which has been extensively used as a basic coating material. The experimental data are correlated with the Henry and Langmuir equations. The Henry's law constants determined in this work are discussed to assess their feasibility as thermodynamic values.

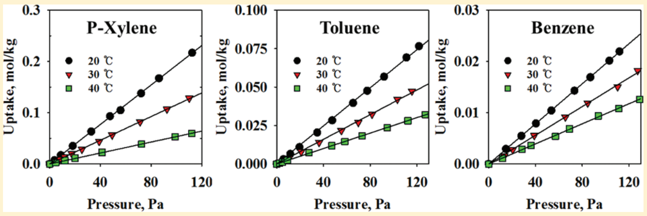

■ INTRODUCTION

Volatile organic compounds (VOCs) are emitted to the atmosphere from fuels, moving vehicles, and also industrial sources, such as solvents, paints, and cleaning agents. The released VOCs can cause harmful effects on human health due to their carcinogenic or toxic characteristics.[1]

Monitoring systems for VOCs have been already introduced and developed in many countries of the world. The concentrations of VOCs are typically determined by using gas chromatography, mass spectrometers, and infrared spectroscopy, etc. These methods have several advantages such as high sensitivity and high selectivity. However, it is not easy to implement them as online measuring systems to obtain individual concentrations in real-time.[2,3] Gas sensors are cheap, simple, and reliable alternative techniques for measuring low-level concentrations directly from mixtures. Among several techniques for gas sensing reported in previous studies, piezoelectric sensors or quartz crystal microbalances (QCMs) have received considerable attention due to their high mass sensitivity.[4−6] The basic principle of QCM is based on the linear relationship between frequency shift and mass change at the crystal surface, as described by Sauerbrey.[7]

A number of porous materials such as activated carbons, zeolites, and molecular imprinting polymers (MIPs) have been successfully used with QCMs in the characterization of VOCs.[8−11] However, the use of porous materials usually demands a binder to attach them onto crystal surfaces. Polyisobutylene (PIB) has been widely used as a binder for coating piezoelectric sensor materials for weakly polar organic species due to its rapid and reversible binding characteristics. The adherent performance of PIB greatly improves the adhesion of fine porous materials on QCM surfaces.[12] However, very little attention has been focused on the adsorption properties of this binder material.

In this study, the adsorption isotherms of VOCs on PIB, which has been traditionally used as a binder material between functional materials and quartz surfaces, are measured at (293.15, 303.15, and 313.15) K in a QCM sensor apparatus. Also, all experimental data are obtained at low pressures to determine the Henry's law constant experimentally. The experimental data are correlated with the Henry and Langmuir equations. The major objective of this work is to assess the Henry's law constants determined as thermodynamic values. In addition to this, the secondary objective is to develop a measuring system to determine the adsorption amounts on nonporous adsorbents with extremely small surface areas such as PIB gels.

Table 1. Basic Properties of Poly(isobutylene)

properties	value	unit
bulk density[a]	0.964	$g \cdot cm^{-3}$
melting point	275	K
solubility parameter[a]	16.5	$(MPa)^{1/2}$
ionization potential	9.24[b]	eV
polarizability	7.987[b]	$\times 10^{-24}$ cm^3

[a] At SATP. [b] Isobutene.

■ EXPERIMENTAL SECTION

Materials. Poly(isobutylene) (PIB, average molecular weight 302 000) was purchased from Fluka. Aromatic compounds such as benzene (99.5 % purity, Junsei Chemical Co.), toluene (99.5 % purity, Junsei Chemical Co.), and *p*-xylene (99.0 % purity, Sigma-Aldrich Co.) were used without further treatment. Their basic properties are summarized in

Received: June 13, 2011
Accepted: January 8, 2012
Published: January 27, 2012

dx.doi.org/10.1021/je2005787 | J. Chem. Eng.Data 2012, 57, 701−707

Table 2. Basic Properties of Benzene, Toluene, and *p*-Xylene

					critical values			
	density	molecular weight	molecular polarizability	ionization potential	T_c	P_c	V_c	Z_c
materials	g·cm^{-3}	g·mol^{-1}	× 10^{-24} cm^3	eV	K	kPa	m^3/kg·mol	-
benzene	0.897	78.11	9.7	9.3	562.1	4895	0.256	0.268
toluene	0.867	92.14	11.53	8.8	591.8	4108	0.316	0.264
p-xylene	0.861	106.16	13.37	8.5	616.2	3511	0.378	0.259

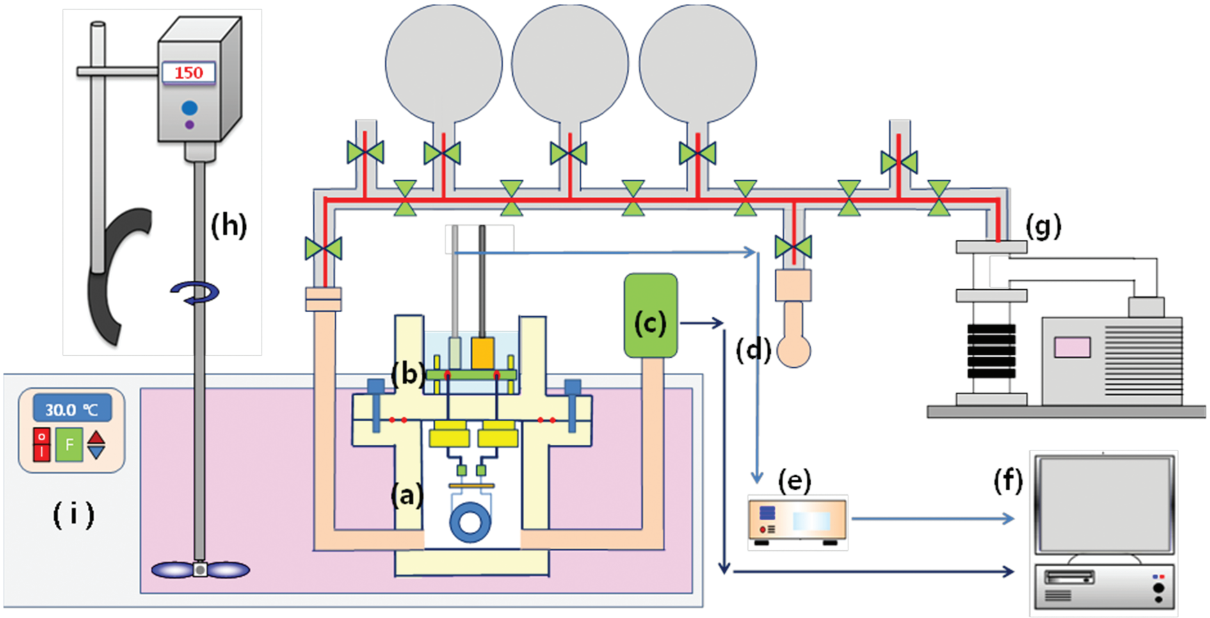

Figure 1. Schematic experimental setup: (a) quartz crystal, (b) oscillator circuit, (c) pressure gauge, (d) liquid sample port, (e) frequency counter, (f) computer, (g) vacuum pump, (h) agitator, and (i) water batch.

Tables 1 and 2. All other reagents are of analytical grade, and ultrapure water is used in preparing all aqueous solutions.

Preparation of PIB-Coated Sensor Elements. AT-cut quartz crystals of 8 MHz (Sunny Electronics, Korea) with Ag electrodes are used as the substrate. The quartz surface is cleaned in diluted piranha solution (the volume ratio, H_2SO_4:H_2O_2, is 3: 1) at 25 °C for 2 min. Subsequently, the crystal is rinsed with distilled water and dried under vacuum conditions. After cleaning up, the quartz surface is coated with 1 wt % PIB/TCE (trichloroethylene) solution using a spin coater at 3000 rpm for 1 min at room temperature. Finally, TCE on the quartz surface is evaporated under vacuum conditions. Then, about 3500 ng of PIB is coated onto the quartz crystal surface.

QCM Sensor Apparatus. A schematic diagram of the QCM sensor apparatus constructed in this work is shown in Figure 1. At a given temperature, vapor is generated in a small vaporization chamber and sent into the first flask, with a volume of about 1 L. After closing the inlet cock and the cock at the neck of the flask, vapor that had remained in the pipe space, which is about 10 mL, was sent into a second flask. According to this operation, the vapor pressure can be reduced to about one hundredth of the pressure of the first flask. Using three steps (three flasks as shown in Figure 1), the vapor pressure can be reduced to about one millionth of the original vapor pressure and is accurately measured by a Baratron absolute pressure transducer (MKS instruments type 690A-13TRA) with a resolution of $1.33 \cdot 10^{-4}$ Pa and an accuracy of ± 0.08 %.

The QCM element is linked to a homemade oscillation circuit and a frequency counter (Agilent 53131A) that is connected to a PC for collecting data. At each equilibrium step, the variation in mass on the quartz surface is quantified by a frequency shift. The decrease in frequency corresponds to the increase in mass on the surface due to the adsorption of certain species. A 1 Hz frequency shift stands for a mass increase of 1.05 ng on the quartz surface in our sensor apparatus. The measurement accuracy of this QCM system is ± 0.02 Hz.

A given amount of PIB is coated on a quartz crystal surface by repeating the coating step mentioned above. After placing the QCM coated with PIB (QCM element) into the adsorption chamber, the chamber is evacuated using a rotary vacuum pump (Edward model RV5) for 6 h at $1.33 \cdot 10^{-1}$ Pa to remove impurities. In the meantime, the adsorption cell is placed in a water bath with a circulator to control the system temperature to within ± 0.05 K. The adsorption amount is measured by the variation of mass (or by frequency shift) in a closed adsorption chamber. The adsorption equilibrium experiments were performed at three different temperatures [(293.15, 303.15, and 313.15) K]. The uncertainty in measuring frequency shifts or adsorption amounts has been checked by experimental errors between three experimental data sets that are separately measured on the same QCM chip. The experimental errors obtained in this work are in the range of (0.1 to 20.0) %, especially large at low pressures. They are shown as error bars on all experimental data in Figure 4.

Characterization. QCM and film surface morphologies are investigated using an atomic force microscope (AFM, XE-100

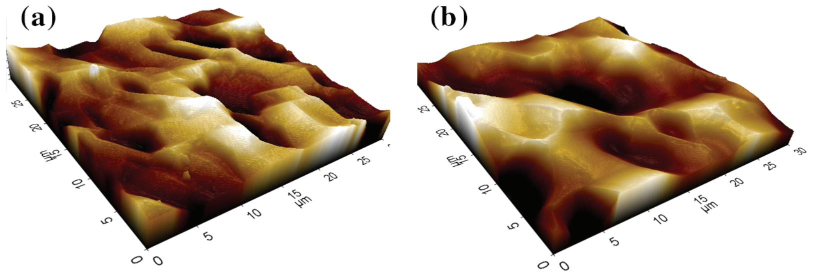

Figure 2. AFM images of bare (a) and PIB-coated (b) QCM surfaces.

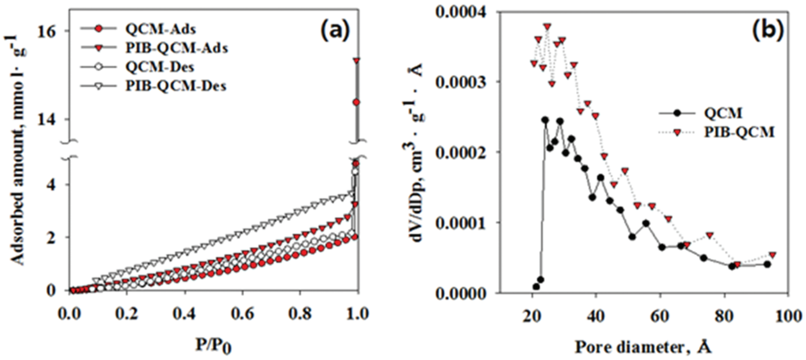

Figure 3. Characterizations of bare and PIB-coated QCMs. (a) The adsorption and desorption of nitrogen at 77 K, and (b) the BJH pore distribution.

from Park System) in tapping mode. Each scan represents a 30 μm × 30 μm lateral area. The root-mean-square (rms) roughness value is also calculated from the AFM images. Furthermore, the specific surface areas of the QCM elements are determined using nitrogen adsorption−desorption isotherms measured at 77 K using a Nano Porosity System (Mirae SI, Korea).

RESULTS AND DISCUSSION

AFM images and nitrogen adsorption isotherms have been used to examine the influence of the PIB-coating process on the QCM surface. A clear difference is noted between bare (panel a) and PIB-coated (panel b) surfaces, as shown in Figure 2. When the mass loading of PIB is 3556 ng, the average film thickness is 80.50 nm. The bare QCM surface has a rough surface with an rms roughness of 334 nm. However, the rms roughness decreases to 107 nm after the PIB-coating process. Figure 3a shows the nitrogen adsorption and desorption isotherms on bare and PIB-coated QCM surfaces at 77 K. The results indicate that the adsorption isotherms are type III or type V, reflecting the weak surface−molecule interactions according to the IUPAC classification.[13] In addition, the mesopore volume distributions evaluated using the Barrett−Joyner−Halenda (BJH) method are shown in Figure 3b. The BET surface area and BJH mesopore volume approximately double due to the PIB-coating process. The average pore sizes of the bare and coated QCM surfaces are (37 and 33) Å, respectively. The overall physical properties of the bare and PIB-coated QCM surfaces are given in Table 1. While the roughness is decreased by the PIB-coating process, the specific surface area and pore volume increase meaningfully as shown in Figure 3 and Table 3. This implies that a certain number of pores exist in the PIB film coated onto the quartz crystal surfaces.

Table 3. Pore Structure Characteristics of Bare and PIB-Coated QCMs

properties	bare QCM	PIB-QCM	unit
BET surface area[a]	2.7	4.9	$m^2 \cdot g^{-1}$
BJH mesopore volume[b]	$4.8 \cdot 10^{-3}$	$7.7 \cdot 10^{-3}$	$cm^3 \cdot g^{-1}$
BJH pore diameter	36.6	33.2	Å

[a]BET ($0.2 < P/P_0 < 0.3$). [b]Desorption branch.

The adsorption equilibrium isotherms of benzene, toluene, and *p*-xylene on the PIB film are obtained at three different temperatures [(293.15, 303.15, and 313.15 K)], and the results are summarized in Figure 4(a−c), respectively. In addition, the adsorption isotherm data are listed in Tables 4 to 6. As shown in Figure 4, the adsorption capacity for *p*-xylene on the PIB film is found to be 0.217 mol·kg⁻¹ at 293.15 K and 112.4 Pa. In the case of toluene, it is 0.077 mol·kg⁻¹ at 293.15 K and 121.7 Pa, and for benzene it is 0.022 mol·kg⁻¹ at 293.15 K and 111.9 Pa. Most experimental data show that the equilibrium adsorption amounts linearly increase with increasing pressure, while they decrease with increasing temperature.

The Langmuir isotherm has been most generally used for pure components.[14] The equation is

$$N = \frac{N_{\max} bP}{1 + bP} \text{ where } b = b_0 \exp\left(-\frac{\Delta H_0}{RT}\right) \tag{1}$$

Here N is the adsorbed amount at pressure P; $N_{\max}$ is the monolayer coverage of the adsorbent surface; and b is the Langmuir adsorption constant, which increases with the binding energy of adsorption and decreases with temperature. The Langmuir isotherm can be reduced to the Henry's law equation when the pressure approaches zero as follows

$$K_L = \lim_{P \to 0} \frac{N}{P} = bN_{\max} \tag{2}$$

Table 4. Adsorption Isotherm Data for *p*-Xylene on PIB Film

293.15 K			303.15 K			313.15 K		
P	ΔF	N	P	ΔF	N	P	ΔF	N
Pa	Hz	$\mathrm{mol\cdot kg^{-1}}$	Pa	Hz	$\mathrm{mol\cdot kg^{-1}}$	Pa	Hz	$\mathrm{mol\cdot kg^{-1}}$
3.866	2.99	$7.540\cdot10^{-3}$	1.200	0.52	$1.320\cdot10^{-3}$	4.800	0.94	$2.380\cdot10^{-3}$
8.799	6.83	$1.722\cdot10^{-2}$	2.725	1.21	$3.060\cdot10^{-3}$	12.00	2.62	$6.620\cdot10^{-3}$
18.27	13.96	$3.523\cdot10^{-2}$	5.415	2.44	$6.150\cdot10^{-3}$	20.00	4.51	$1.139\cdot10^{-2}$
32.80	25.09	$6.331\cdot10^{-2}$	11.87	5.36	$1.351\cdot10^{-2}$	41.33	8.93	$2.252\cdot10^{-2}$
47.60	36.96	$9.324\cdot10^{-2}$	17.47	7.98	$2.013\cdot10^{-2}$	72.53	15.33	$3.868\cdot10^{-2}$
55.86	41.58	$1.049\cdot10^{-1}$	39.06	17.43	$4.397\cdot10^{-2}$	98.93	20.90	$5.272\cdot10^{-2}$
72.13	54.60	$1.378\cdot10^{-1}$	49.33	22.36	$5.642\cdot10^{-2}$	112.0	23.62	$5.960\cdot10^{-2}$
86.26	66.25	$1.672\cdot10^{-1}$	71.33	32.55	$8.212\cdot10^{-2}$			
112.4	85.99	$2.170\cdot10^{-1}$	92.53	42.42	$1.070\cdot10^{-1}$			
			110.1	50.82	$1.282\cdot10^{-1}$			

Table 5. Adsorption Isotherm Data for Toluene on PIB Film

293.15 K			303.15 K			313.15 K		
P	ΔF	N	P	ΔF	N	P	ΔF	N
Pa	Hz	$\mathrm{mol\cdot kg^{-1}}$	Pa	Hz	$\mathrm{mol\cdot kg^{-1}}$	Pa	Hz	$\mathrm{mol\cdot kg^{-1}}$
5.733	1.08	$3.140\cdot10^{-3}$	8.266	0.96	$2.780\cdot10^{-3}$	2.533	0.21	$6.100\cdot10^{-4}$
11.60	2.26	$6.560\cdot10^{-3}$	10.40	1.21	$3.510\cdot10^{-3}$	4.933	0.42	$1.220\cdot10^{-3}$
19.47	3.78	$1.099\cdot10^{-2}$	20.93	2.71	$7.870\cdot10^{-3}$	9.066	0.84	$2.440\cdot10^{-3}$
34.66	7.04	$2.045\cdot10^{-2}$	36.26	4.82	$1.400\cdot10^{-2}$	27.60	2.52	$7.330\cdot10^{-3}$
47.46	9.76	$2.838\cdot10^{-2}$	55.33	7.47	$2.170\cdot10^{-2}$	47.20	4.09	$1.190\cdot10^{-2}$
65.33	13.65	$3.968\cdot10^{-2}$	69.86	9.29	$2.700\cdot10^{-2}$	58.26	5.04	$1.465\cdot10^{-2}$
77.46	16.38	$4.761\cdot10^{-2}$	81.59	11.11	$3.230\cdot10^{-2}$	73.06	6.30	$1.831\cdot10^{-2}$
91.86	19.53	$5.677\cdot10^{-2}$	103.3	14.48	$4.210\cdot10^{-2}$	94.53	8.08	$2.350\cdot10^{-2}$
111.1	23.83	$6.928\cdot10^{-2}$	115.7	16.31	$4.740\cdot10^{-2}$	112.3	9.66	$2.808\cdot10^{-2}$
121.7	26.36	$7.661\cdot10^{-2}$				127.2	11.03	$3.205\cdot10^{-2}$

Table 6. Adsorption Isotherm Data for Benzene on PIB Film

293.15 K			303.15 K			313.15 K		
P	ΔF	N	P	ΔF	N	P	ΔF	N
Pa	Hz	$\mathrm{mol\cdot kg^{-1}}$	Pa	Hz	$\mathrm{mol\cdot kg^{-1}}$	Pa	Hz	$\mathrm{mol\cdot kg^{-1}}$
14.69	0.86	$2.940\cdot10^{-3}$	13.47	0.47	$1.580\cdot10^{-3}$	11.87	0.31	$1.080\cdot10^{-3}$
27.95	1.60	$5.480\cdot10^{-3}$	20.53	0.82	$2.770\cdot10^{-3}$	28.40	0.84	$2.880\cdot10^{-3}$
40.40	2.31	$7.920\cdot10^{-3}$	38.93	1.64	$5.540\cdot10^{-3}$	36.26	1.05	$3.600\cdot10^{-3}$
53.60	3.04	$1.044\cdot10^{-2}$	65.55	2.70	$9.130\cdot10^{-3}$	57.06	1.57	$5.400\cdot10^{-3}$
73.35	4.17	$1.430\cdot10^{-2}$	84.66	3.51	$1.188\cdot10^{-2}$	69.06	1.99	$6.840\cdot10^{-3}$
86.93	4.93	$1.692\cdot10^{-2}$	110.4	4.45	$1.505\cdot10^{-2}$	93.73	2.73	$9.360\cdot10^{-3}$
103.2	5.88	$2.016\cdot10^{-2}$	127.5	5.38	$1.822\cdot10^{-2}$	111.3	3.15	$1.080\cdot10^{-2}$
111.9	6.40	$2.196\cdot10^{-2}$				129.1	3.67	$1.260\cdot10^{-2}$

Table 7. Parameters of Henry and Langmuir Isotherms

	T	Henry's law		Langmuir isotherm			
adsorbate	K	K_H, $\mathrm{mol\cdot kg^{-1}\cdot kPa^{-1}}$	R^{2a}	K_L, $\mathrm{mol\cdot kg^{-1}\cdot kPa^{-1}}$	N_{max}, $\mathrm{mol\cdot kg^{-1}}$	b, $\mathrm{kPa^{-1}}$	R^{2a}
benzene	293.15	0.195	1.000	0.195	$3.899\cdot10^{-5}$	$5.004\cdot10^{3}$	0.999
	303.15	0.140	0.998	0.140	$1.576\cdot10^{-2}$	$8.903\cdot10^{0}$	0.998
	313.15	0.098	0.999	0.099	$6.559\cdot10^{-2}$	$1.504\cdot10^{0}$	0.998
toluene	293.15	0.615	0.999	0.619	$3.335\cdot10^{-5}$	$1.857\cdot10^{4}$	0.999
	303.15	0.401	0.998	0.402	$1.035\cdot10^{-2}$	$3.881\cdot10^{1}$	0.998
	313.15	0.251	1.000	0.253	$7.553\cdot10^{-2}$	$3.348\cdot10^{0}$	0.998
p-xylene	293.15	1.926	1.000	1.927	$1.885\cdot10^{-4}$	$1.022\cdot10^{4}$	0.999
	303.15	1.155	1.000	1.159	$3.432\cdot10^{-2}$	$3.376\cdot10^{1}$	0.999
	313.15	0.534	1.000	0.551	$3.327\cdot10^{-1}$	$1.655\cdot10^{0}$	0.999

[a] Square correlation coefficient.

The Henry's law constant is an important parameter for accurate thermodynamic analyses.[15] The isotherm parameters for the Langmuir isotherm and the Henry's law constants are listed in Table 7. The Henry's law constant, K_H, is directly obtained from the slope of the isotherm shown in Figure 4, while the other Henry's law constant, K_L, is calculated using eq 2 with the Langmuir isotherm parameters, b and N_{max}. It is noted that both values given in Table 7 are quite similar, which implies that the experimental conditions are near the Henry's law region. On the other hand, the Henry's law constants of the three aromatic components on the PIB film decrease with temperature. This is a natural result in physical adsorption cases.[16,17] Henry's law plots for benzene, toluene, and p-xylene on the PIB film at 303.15 K are shown in Figure 5(a). The flat lines in this figure prove that the Henry's law constants can be experimentally obtained using the apparatus with an adsorption cell on a quartz crystal microbalance. In addition, Figure 5(b) shows the Henry's law constant (K_H) for three aromatic species at three different temperatures. The adsorption affinity to the PIB film increases in the order benzene < toluene < p-xylene.

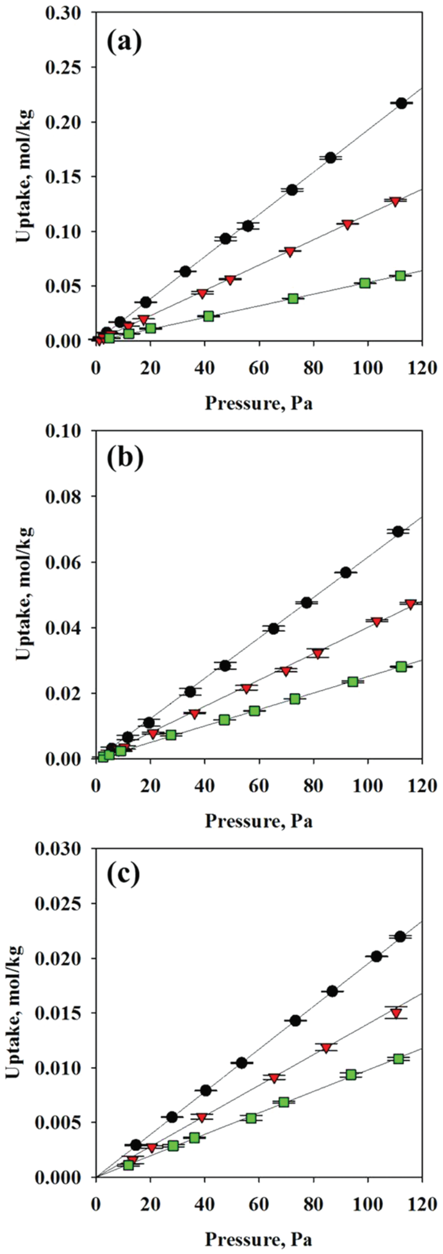

Figure 4. Adsorption isotherms of p-xylene (a), toluene (b), and benzene (c) on PIB film: (●), 293.15 K; (▼), 303.15 K; (■), 313.15 K. Solid lines denote predictions using Henry's isotherm.

The Clausius–Clapeyron equation was used to obtain the isosteric heat of adsorption for aromatic hydrocarbons. The equation has the following form

$$\frac{q_{st}}{RT^2} = \left[\frac{\partial \ln P}{\partial T}\right]_N \tag{3}$$

where P is pressure; T is temperature; R is the gas constant; and N is the amount of material adsorbed. Figure 6(a) shows the isosteric heat of adsorption versus the adsorbed amount. As shown in this figure, the values for the isosteric heat obtained from the adsorption curves are almost constant in terms of the loading in the region of measurement.[18] This result shows that the adsorbent has an energetically homogeneous surface for benzene, toluene, and xylene. The order of isosteric heats of adsorption are p-xylene (37.9 kJ·mol^{-1}) > toluene (31.9 kJ·mol^{-1}) > benzene (24.7 kJ·mol^{-1}).

The molecular interaction forces between adsorbate molecules and noncharged adsorbent surfaces (i.e., polymer materials) can be obtained by the following 10–4 potential equation.[19]

$$\varphi_{1,\mathrm{SLP}} = \frac{10\varepsilon^*_{1,\mathrm{SLP}}}{3}\left[\frac{1}{5}\left(\frac{\sigma_{12}}{z}\right)^{10} - \frac{1}{2}\left(\frac{\sigma_{12}}{z}\right)^{4}\right] \tag{4}$$

where $\varphi_{1,\mathrm{SLP}}$ is the potential energy of a single lattice plane (SLP); σ_{12} is the collision diameter; and z is the distance between the molecule and the lattice plane. The minimum potential energy, $\varepsilon^*_{1,\mathrm{SLP}}$, between a molecule and a single lattice plane is

$$\varepsilon^*_{1,\mathrm{SLP}} = \frac{6}{5}\pi n \varepsilon^*_{12}\sigma^2_{12} \tag{5}$$

Here n is the number of the interacting centers per unit area of the lattice plane, and ε^*_{12} is the minimum adsorption potential that may be a function of polarizability and ionization potential of molecules involved. In this work, the Lorentz–Betherlot rule is used to calculate σ_{12} and ε^*_{12}. To calculate the number of the interacting centers per unit area, it is assumed that the lattice layer of PIB has the hexagonal structure. The parameters used in calculations are summarized in Table 8, together with the isosteric heats of adsorption previously obtained in this work.

The minimum adsorption potential energies for benzene, toluene, and p-xylene are (26.3, 28.9, and 31.1) kJ·mol^{-1}, respectively, which are almost identical to the isosteric heats of adsorption as shown in Table 8. It should be noted that two values for benzene are smaller than those for other aromatic molecules having methyl groups. Previous reports have shown that the adsorption affinities of aromatic compounds are highly dependent on their molecular polarizabilities and first ionization potentials.[20−22] Owing to the number of electrons for polarization, the molecular polarizability generally increases with the molecular weights, and it may contribute to the adsorption affinity eventually because of the increase in the adsorption potential energy. As shown in Figure 6(b), the isosteric heat of adsorption has close relationships with physical properties such as first ionization potential and molecular polarizability.

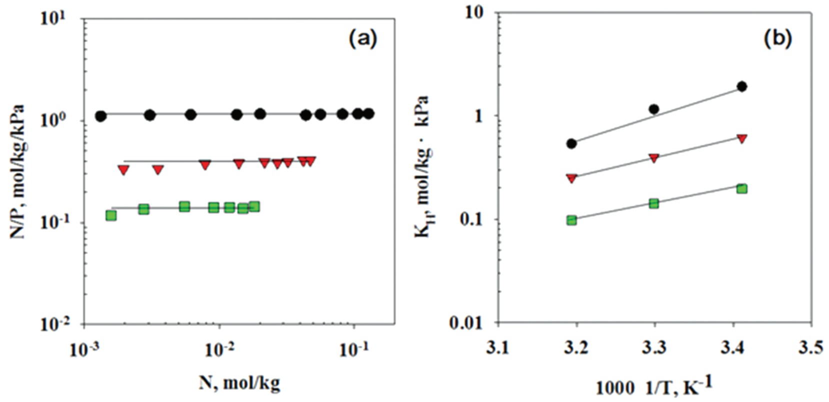

Figure 5. (a) Henry's law plot at 303.15 K and (b) Henry's law constant (K_H) at different temperatures for *p*-xylene, toluene, and benzene on PIB film: (●), p-xylene; (▼), toluene; (■), benzene.

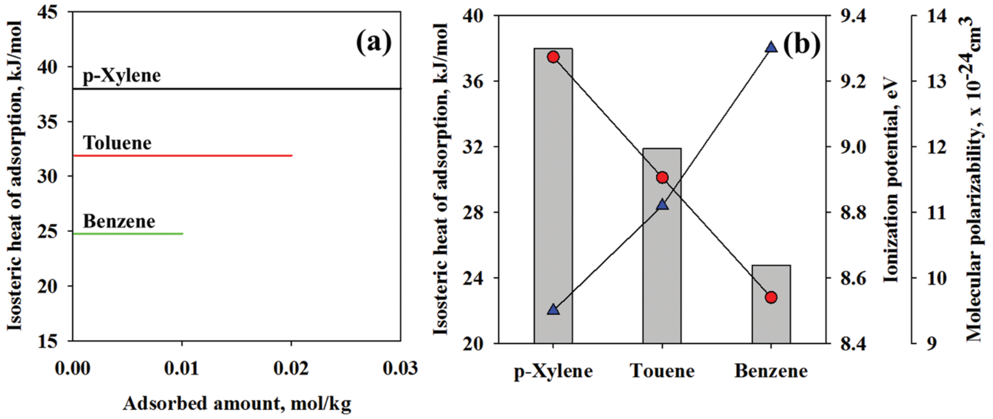

Figure 6. (a) Isosteric heats of adsorption from the Langmuir isotherm as a function of loading and (b) the relation between isosteric heat of adsorption and physical properties of adsorbate: bar, Isosteric heat of adsorption; ▲, first ionization potential; ●, molecular polarizability.

Table 8. Potential Parameters and Energy Values of Chemicals

	ε_{12}^*	σ_{12}	$\varepsilon_{1,\mathrm{SLP}}^{*}$ [a]	q_{st} [b]
materials	J·molecule^{-1}	nm	kJ·mol^{-1}	kJ·mol^{-1}
benzene	$4.004 \cdot 10^{-21}$	0.560	26.3	24.7
toluene	$3.993 \cdot 10^{-21}$	0.587	28.9	31.9
p-xylene	$3.939 \cdot 10^{-21}$	0.614	31.1	37.9

[a] Minimum adsorption potential energy. [b] Isosteric heat of adsorption.

■ CONCLUSIONS

Low-pressure adsorption isotherms of benzene, toluene, and *p*-xylene on PIB gel are experimentally measured at (293.15, 303.15, and 313.15) K in an adsorption cell with a QCM. Two different Henry's law constants for three VOC vapors are obtained from Henry's law plots and Langmuir isotherm parameters, respectively. It is found that the two values obtained are practically the same, which implies that the experimental conditions are very near the Henry's law region. There are two important results in this work. First Henry's law constants can be experimentally obtained using a QCM-based adsorption system; the system may be used in analyzing given adsorption systems theoretically. The second result is that one can simply conduct adsorption equilibrium experiments even on gel-type polymers that have very low adsorption capacities using this experimental system.

■ AUTHOR INFORMATION

Corresponding Author

*Tel.: +82-62-530-1877. E-mail address: hmoon@jnu.ac.kr.

Funding

This work was supported by National Research Foundation of Korea Grant funded by the Korean Government (No. 2010-0028085).

■ REFERENCES

(1) Beauchet, R.; Magnoux, P.; Mijoin, J. Catalytic oxidation of volatile organic compounds (VOCs) mixture (isopropanol/o-xylene) on zeolite catalysts. *Catal. Today* **2007**, *124*, 118−123.

(2) Matsuguchi, M.; Uno, T.; Aoki, T.; Yoshida, M. Chemically modified copolymer coatings for mass-sensitive toluene vapor sensors. *Sens. Actuators, B* **2008**, *131*, 652−659.

(3) Balathanigaimani, M. S.; Shim, W. G.; Lee, M. J.; Lee, J. W.; Moon, H. Adsorption Isotherms of Benzene and Toluene on Corn Grain-Based Carbon Monolith at (303.15, 313.15, and 323.15) K. *J. Chem. Eng. Data* **2008**, *53*, 732−736.

(4) Levi, M. D.; Salitra, G.; Levy, N.; Aurbach, D.; Maier, J. Application of a quartz-crystal microbalance to measure ionic fluxes in microporous carbons for energy storage. *Nat. Mater.* **2009**, *8*, 872−875.

(5) Abe, T.; Esashi, M. One-chip multichannel quartz crystal microbalance (QCM) fabricated by Deep RIE. *Sens. Actuators, A* **2000**, *82*, 139−143.

(6) Bai, H.; Shi, G. Gas sensors based on conducting polymers. *Sensors* **2007**, *7*, 267−307.

(7) Sauerbrey, G. The use of quartz oscillators for weighing thin layers and for microweighing. *Z. Phys.* **1959**, *155*, 206−222.

(8) Sasaki, I.; Tsuchiya, H.; Nishioka, M.; Sadakata, M.; Okubo, T. Gas sensing with zeolite-coated quartz crystal microbalances − principal component analysis approach. *Sens. Actuators, B* **2002**, *86*, 26−33.

(9) Kikuchi, M.; Tsuru, N.; Shiratori, S. Recognition of terpenes using molecular imprinted polymer coated quartz crystal microbalance in air phase. *Adv. Mater.* **2006**, *7*, 156−161.

(10) Lu, H. H.; Rao, Y. K.; Wu, T. Z.; Tzeng, Y. M. Direct characterization and quantification of volatile organic compounds by piezoelectric module chips sensor. *Sens. Actuators, B* **2009**, *137*, 741−746.

(11) Si, P.; Mortensen, J.; Komolov, A.; Denborg, J.; Møller, P. J. Polymer coated quartz crystal microbalance sensors for detection of volatile organic compounds in gas mixtures. *Anal. Chim. Acta* **2007**, *597*, 223−230.

(12) McGill, R. A.; Abraham, M. H.; Gate, J. W. Choosing Polymer Coatings for Chemical Sensors. *CHEMTECH* **1994**, *9*, 27−37.

(13) Rouquerol, F.; Rouquerol, J.; Kenneth, S. *Adsorption by Powders and Porous Solids*; Academic Press: London, 1999.

(14) De Boer, J. H. *The Dynamical Character of Adsorption*; Clarendon Press: Oxford, 1970.

(15) Borkar, C.; Tomar, D.; Gumma, S. Adsorption of Dichloromethane on Activated Carbon. *J. Chem. Eng. Data* **2010**, *55*, 1640−1644.

(16) Drago, S.; Webster, C. E.; McGilvray, J. M. A multiple-process equilibrium analysis of silica gel and HZSM-5. *J. Am. Chem. Soc.* **1998**, *120*, 538−547.

(17) Tarun, K.; Poddar.; Kamalesh, K. Sirkar. Henry's Law Constant for Selected Volatile Organic Compounds in High-Boiling Oils. *J. Chem. Eng. Data* **1996**, *41*, 1329−1332.

(18) Sircar, S. Heat of adsorption on heterogeneous adsorbents. *Appl. Surf. Sci.* **2005**, *252*, 647−653.

(19) Do, D. D., *Adsorption Analysis: Equilibria and Kinetics*; Imperial College Press: Singapore, 1998.

(20) Shim, W. G.; Kim, S. C. Heterogeneous adsorption and catalytic oxidation of benzene, toluene and xylene over spent and chemically regenerated platinum catalyst supported on activated carbon. *Appl. Surf. Sci.* **2010**, *256*, 5566−5571.

(21) Kim, S. C.; Shim, W. G. Properties and performance of Pd based catalysts for catalytic oxidation of volatile organic compounds. *Appl. Catal., B* **2009**, *92*, 429−436.

(22) Geng, Q.; Chen, N. Photocatalytic degradation of a gaseous benzene-toluene mixture in a circulated photocatalytic reactor. *Chem. Eng. Technol.* **2011**, *34*, 400−408.